

Accurate measurement of muscle belly length in the motion analysis laboratory: potential for the assessment of contracture

N.R. Fry, C.R. Childs, L.C. Eve, M. Gough, R.O. Robinson, A.P. Shortland*

One Small Step Gait Laboratory, Thomas Guy House, Guy's Hospital, London SE1 9RT, UK

Received 26 January 2002; received in revised form 29 April 2002; accepted 7 May 2002

Abstract

Two-dimensional ultrasound imaging was combined with motion analysis technology to measure distances between remote anatomical landmarks. The length of the belly of the medial gastrocnemius muscle in five normal adults (nine limbs) was estimated using this technique. Our results *in vivo* were similar to the reported data for the lengths of muscles in cadavers, and were consistent with the expected relationship between muscle belly length and ankle joint angle. Experiments *in vitro* demonstrated that the accuracy of the device was better than 2 mm over 20 cm. Measurements on the same subject on different occasions showed that the results were repeatable *in vivo*. Rendering of the reconstructed volume of a foam phantom gave results comparable to photographic images. This validated technique could be used to measure muscle lengths in children with spastic cerebral palsy and indicate which muscles had fixed shortening, and to what extent.

© 2002 Elsevier Science B.V. All rights reserved.

Keywords: Ultrasound; Muscle morphology; Cerebral palsy

1. Introduction

Children with spastic cerebral palsy (CP) often develop fixed shortening of some of the muscles of the lower limb. A number of management options are available which include injections of Botulinum toxin to relieve the dynamic component of shortening [1], physiotherapy and serial casting [2] to alleviate mild contractures and soft tissue surgery to correct more severe contractures [3]. Since the affected muscles in spastic CP may progress rapidly from dynamic to fixed shortening, management involves an accurate identification of the individual muscles requiring treatment and selection of the most appropriate treatment for the child. At present, there are no simple tools to measure muscle length directly. Indirect measurement consists of clinical examination of joint ranges but this is subject to a number of systematic and random errors that include intra- and inter-rater errors and variability in goniometric measurement [4] and patient tone. It is also difficult to determine which muscles within a group acting at a particular joint are responsible for stiffness at that joint. Manual assessment of neuromuscular strength is another clinical measure but unfortunately, this technique does not distinguish between selective muscle control and the mechanical potential of muscles.

Computed tomography (CT) or magnetic resonance imaging (MRI) can be used to measure muscle dimensions. However, these techniques are expensive, may not be available locally, do not readily allow repositioning of the joints and the subjects may require sedation. CT poses the additional problem of exposure to high-energy radiation.

Muscle and tendon are easily visualised with B-mode ultrasound imaging. However, the image window is rarely large enough to visualise the whole length of the muscles of interest within the lower limb. 3D ultrasound systems do exist but most of the commercially available devices have a limited field of view suitable for foetal imaging but less appropriate to musculo-skeletal applications. Competing 'freehand' technologies exist for reconstructing volume data over large sweeps of the ultrasound probe. Image correlation techniques can be

muscle and tendon are easily visualised with B-mode ultrasound imaging. However, the image window is rarely large enough to visualise the whole length of the muscles of interest within the lower limb. 3D ultrasound systems do exist but most of the commercially available devices have a limited field of view suitable for foetal imaging but less appropriate to musculo-skeletal applications. Competing 'freehand' technologies exist for reconstructing volume data over large sweeps of the ultrasound probe. Image correlation techniques can be

* Corresponding author. Tel.: +44-20-795-52339; fax: +44-20-795-52340

E-mail address: adam.shortland@gstt.sthames.nhs.uk (A.P. Shortland).

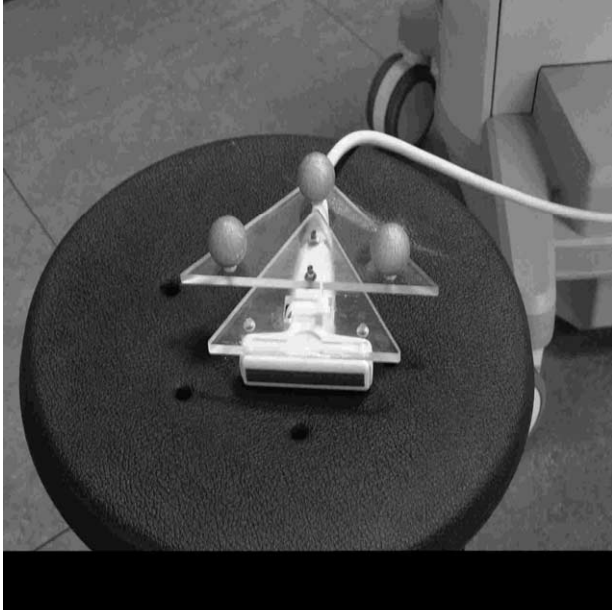


Fig. 1. Reflective markers mounted in a Perspex™ frame attached to an ultrasound probe.

used to align adjacent 2D images. An alternative is to attach a magnetic positional sensor to an ultrasound probe. The position and attitude of the sensor within a supplied magnetic field is associated by a computer with the coincident video frame. Systems employing magnetic sensors have good spatial resolution [5] but measurements may suffer distortions in the presence of metal capable of containing significant eddy currents. Another approach is optical tracking of the ultrasound probe. Gait laboratories often have motion analysis equipment available that could perform this task. Here, we detail a method to measure distances between remote anatomical landmarks within subjects using an optically tracked ultrasound probe.

2. Methods

Three reflective spherical markers (25 mm diameter) were mounted on a Perspex™ frame that could be attached rigidly to a linear array ultrasound probe (UST-5710-7.5 Linear Array, Aloka, Japan) (Fig. 1). We use our laboratory motion analysis system (Vicon 370, Vicon Motion Systems, Oxford, UK) with three infrared cameras mounted on tripods to provide an analysis volume of approximately $1.0 \times 0.5 \times 0.5 \text{ m}^3$. The video output (CCIR, composite) of our ultrasound machine (SSD-1000, Aloka, Japan) was connected to a frame grabber (Broadway Pro, DataTranslation Inc., USA) that was operated synchronously with the marker data collection. In this way, each video frame from the ultrasound device had an associated position and attitude defined by the reflective markers.

The laboratory co-ordinate system was defined by the placement of a calibration frame (clinical L-frame device, Vicon 370) during calibration of the analysis volume. The probe co-ordinate system was defined by the probe markers. The ultrasound image co-ordinate system was defined as having its origin at the top left hand corner of the image with orthogonal axes along its horizontal and vertical excursion. The transformation, \mathbf{T}_c , of a point in image space to a point in probe space was informed by a calibration procedure (see below). The transformation mapping a point in probe space to a point in the laboratory co-ordinate system, \mathbf{T}_p , was informed by the position and orientation of the three reflective markers. In this way, a point in the image plane $\langle u, v \rangle$ was mapped to a point in laboratory co-ordinate space $\langle x, y, z \rangle$ by the transformation given in Eq. (1).

$$\begin{pmatrix} x \\ y \\ z \\ 1 \end{pmatrix} = \mathbf{T}_p \mathbf{T}_c \begin{pmatrix} S_u u \\ S_v v \\ 0 \\ 1 \end{pmatrix}, \quad (1)$$

where \mathbf{T}_c and \mathbf{T}_p are quaternion matrices, and S_u and S_v are image scaling factors.

2.1. Calibration procedures

Each of the two transformations required its own calibration. Calibration of the analysis volume was similar to the standard Vicon method. It consisted of a static calibration that fixed the origin and orientation of the analysis volume and a dynamic calibration that employed a wand consisting of two 25 mm diameter markers separated by 114 mm. The wand was slowly waved through the analysis volume. The software calculated an error value indicating the level of accuracy associated with each camera. The calibration was accepted if the error values were all less than 0.4 mm. If they were not, the calibration was repeated to ensure that the calibration objects were in the field of view at all times during calibration. This may have required adjustment of camera position.

The transformation, \mathbf{T}_c , was informed by a separate calibration procedure. A single cross-wire, made from needle worker's thread, mounted in a water tank was imaged from many different directions [6]. We used an optimisation routine (Nelder-Mead simplex direct search [7]) to solve for the set of nine unknown parameters in Eq. (1) (S_u and S_v were found using a standard 2D ultrasound calibration phantom), so that an error function, the root-mean squared error (RMSE), of all the estimates was minimised. The minimisation algorithm was restarted using different initial values of the parameters to add confidence to the final parameter estimation. A further test of validity was made by mounting two cross-wires within the water tank a

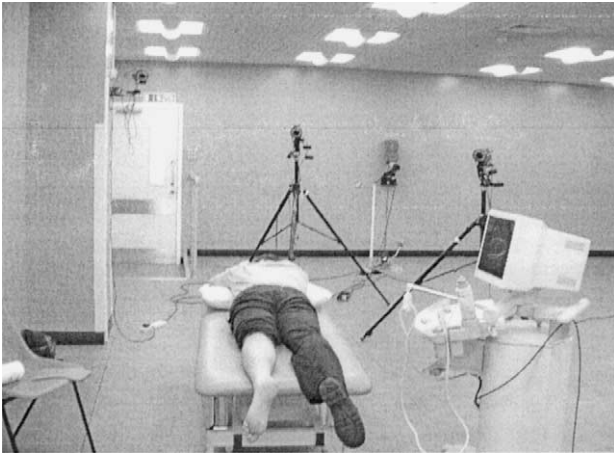


Fig. 2. Typical configuration of subject, ultrasound machine and motion analysis cameras during data collection.

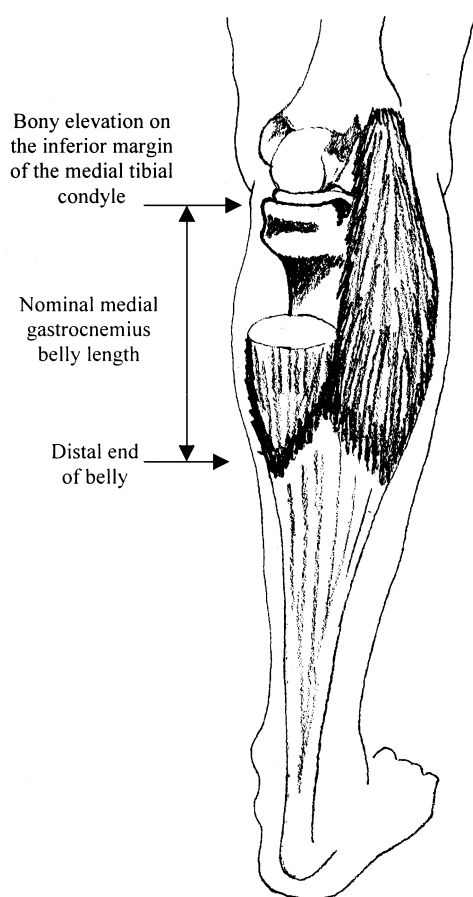


Fig. 3. Illustration of the anatomical landmarks for the measurement of nominal medial gastrocnemius belly length. Adapted from 'Anatomy and figure drawing' [17].

known distance apart (202 mm). Both cross-wires were imaged, their positions in laboratory space computed and the distance between them calculated.

2.2. Subjects

The subjects were five healthy adults (three males, two females, mean age 36.2 years, range 24.5–52.0 years). Data was collected from both legs of four of the subjects and only the left leg of the fifth. The subjects reported no musculoskeletal or neurological problems associated with the lower limbs.

2.3. Data collection

The subjects lay prone on the plinth positioning their ankles level with the end of the plinth and their knees fully extended (Fig. 2). The ultrasound probe was manipulated to generate a sequence of transverse images, one every 0.04 s, from the calcaneum, along the Achilles tendon and the medial gastrocnemius belly as far as the femoral condyles. Video images from the ultrasound machine were recorded with the framegrabber synchronised to our motion analysis system. Images representing the distal point of the medial gastrocnemius muscle belly and a posterior bony elevation on the inferior aspect of the medial tibial condyle were selected. The distance between these points in the images was calculated using the transformation informed by the calibration procedure and is referred to as the nominal muscle belly length (Fig. 3). Measurements of resting ankle angle, (the angle assumed by the ankle joint in the absence of external forces), maximum passive plantarflexion and dorsiflexion range were made. Manual goniometry was used to record the angle made by the lateral border of the hind foot and the principal axis of the leg. Data collection was repeated with the ankle held at its natural resting angle, at maximum plantarflexion, maximum dorsiflexion and at appropriate intermediate angles.

The data collection was repeated for the resting ankle angle in one subject on four different occasions over a period of 9 months.

3. Results

The *in vitro* (single cross-wire) calibration procedure produced values for RMSE of less than 1.5 mm repeatedly. The maximum error of location in any of the images ($N = 25$) collected for the calibration procedure was 2.6 mm. There was a small systematic error in the estimation of distance between two cross-wires, 202 mm apart in the analysis volume. The ultrasound technique repeatedly ($N = 5$) overestimated this distance by 1.4 ± 1.3 mm (mean \pm 1 S.D.). The repeated measurements made of medial gastrocnemius muscle length of one subject at his resting ankle angle produced results in the range 203–205 mm.

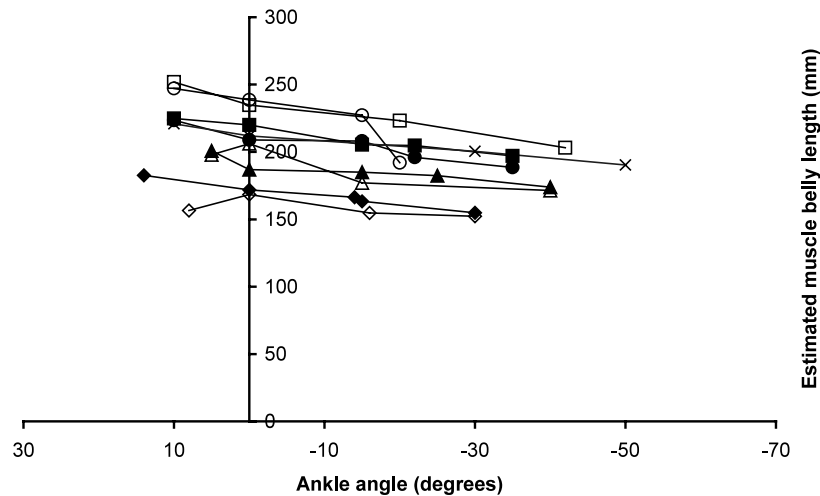


Fig. 4. The relationship between estimated medial gastrocnemius belly length and ankle joint angle. Individual subjects are identified by unique symbols. Closed symbols indicate left lower limb. Open symbols indicate right lower limb.

Fig. 4 depicts the relationship between ankle joint angle and nominal medial gastrocnemius belly length. As might be expected, the length of the muscle reduced with increasing plantarflexion.

4. Discussion

We have described a technique to measure anatomical distances non-invasively, integrating the technology available in most movement laboratories with an inexpensive ultrasound scanner. The method is accurate to within a few millimetres over typical muscle dimensions in the lower limb, and results are repeatable *in vivo*. Our muscle length measurements are similar to those made from adult cadavers [8,9] and consistent with the expected relationship between length and joint angle.

4.1. Limitations of the study

In this study, we measured a nominal muscle length, the distance between the distal end of the medial gastrocnemius muscle belly and the posterior bony elevation on the inferior margin of the medial tibial condyle. These landmarks were chosen because their identification under ultrasound scanning is straightforward. The proximal end of the gastrocnemius is difficult to visualise because of the complex of overlapping muscle and tendon that cross the posterior aspect of the knee joint.

We used a linear array probe to perform a transverse scan of the calf musculature. These probes have relatively poor resolution in a direction perpendicular to the ultrasound image plane (direction of elevation) that is typically 1 mm, though this depends on the distance from the probe face. New ultrasound probe

technologies (Multi-D™, Siemens Gmbh) developed recently have improved resolution in the direction of elevation, by introducing a 2D array of elements onto the probe surface to enable improved focussing of the ultrasound beam. The spatial and temporal resolution of our camera system may also be improved with increased charge-coupled device (CCD) element density and higher frame rates.

The video outputs of our ultrasound system and our motion capture cameras were not genlocked (synchronised to available pulses within the composite video signal). Temporal errors of up to 0.04 s may have been incurred. At a typical scanning speed this equates to a location error in the direction of the ultrasound scan of 0.5 mm. In practice, the error will be smaller than this because we computed the distance between landmarks, and the operator, NRF, scanned at a steady velocity.

During scanning, we were unable to assess the activity status of the underlying musculature with electromyographic recordings. Increased muscle tone may have influenced our muscle length measurements. Recordings from the lateral compartment of the gastrocnemius would be possible while the medial compartment was scanned.

4.2. Clinical implications

The active and passive mechanical performance of muscles depends upon muscle architecture and morphology [10]. The magnitude of force production is proportional to physiological cross-sectional area (PCSA), while fibre length is a determinant of the speed of shortening. A small body of work has been devoted to the study of muscle morphology and architecture in human cadavers [8,9], and recently in live adult subjects using both ultrasound [11,12] and MRI [13]. However, little is known of the architecture of muscles in children

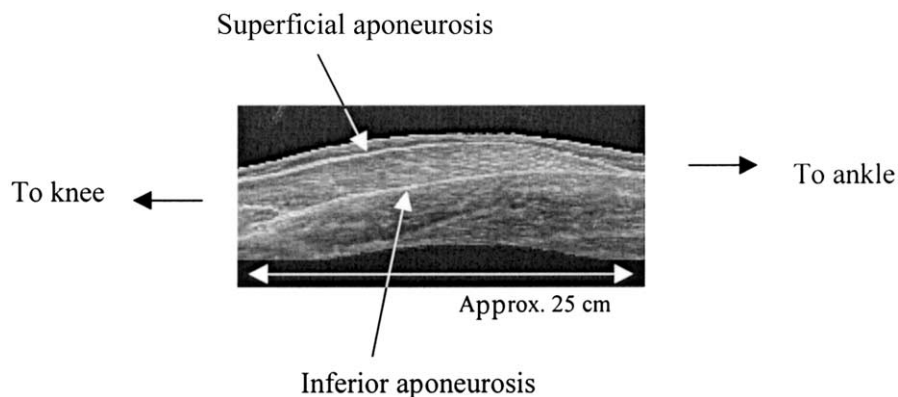


Fig. 5. Longitudinal slice through a 3D volumetric ultrasound scan of the medial gastrocnemius of a normal adult.

and specifically those with spastic CP. Muscle function is difficult to evaluate by direct means in children with CP although some studies have been performed using servomotor systems to measure moment–angle relationships [2]. Measuring the active properties of the muscle groups around a joint such as the force generated by maximum voluntary contraction requires good muscle selectivity and joint stability, attributes that may not be present in the subject with spastic CP.

Until recently, it was widely believed by clinicians that the short muscles observed in children with spastic CP are due to a reduction in muscle fibre length [14]. However, quantitative measurements of these muscle dimensions using 2D ultrasound indicate that fibre shortening is not responsible for muscle contracture, at least in the medial gastrocnemius of children with spastic diplegia [15]. Three-dimensional studies of muscle morphology may change our perspective on the causes and pathology of fixed muscle shortening.

There is a need to quantify the effect of focal interventions on muscle architecture and function when attempting to improve muscle length. This may help to predict clinical outcomes better. With this tool, we are in a position to document the morphological changes in muscle and hence explain the effects of surgery and other interventions on the function of muscle.

4.3. Future developments

Although the ultrasound images collected by the method described here are non-uniformly orientated, a structured 3D array of voxels can be constructed. A number of suitable algorithms exist but the most commonly used is the voxel nearest neighbour interpolation, in which the value of a voxel is made equal to the value of the nearest pixel within the original image sequence [16]. The volume produced can be ‘resliced’ so that image planes not available from 2D ultrasound scanning can be realised (Fig. 5). Measurements of muscle volume can be made with standard segmentation

techniques, and fascicle length and pennation angle can be computed at any point. The reconstructed volume can be processed to produce photo-realistic images of 3D structures (Fig. 6).

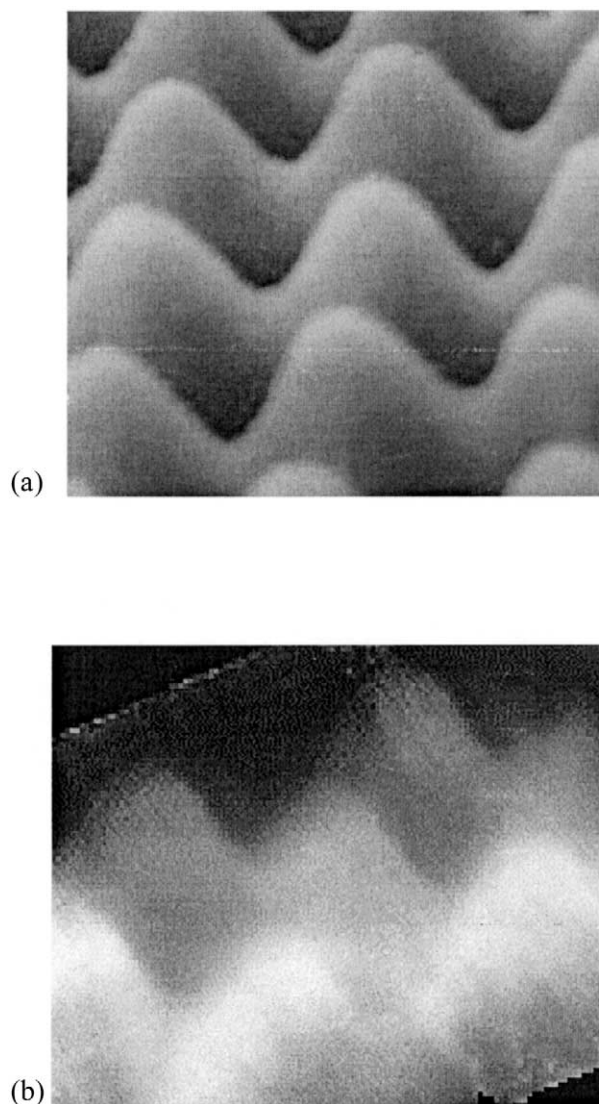


Fig. 6. (a) Photographic image; and (b) volume-rendered 3D ultrasound image of packing foam.

5. Conclusion

We have described and validated a technique to measure the distance between remote anatomical landmarks using optical-tracking of an ultrasound probe. The technique is applicable to the measurement of muscle belly lengths in patients with neuromuscular problems that result in muscle contracture.

Acknowledgements

Ms Nicola Fry was funded by a grant from the Wishbone Trust supported by the Hudson Foundation, The Clothworkers Foundation, the London Law Trust and the Harold Wingate Foundation. The ultrasound scanner used in this work was funded by the The Charitable Foundations of Guy's & St Thomas' Hospital, and the One Small Step Charitable Trust.

References

- [1] Koman A, Mooney JF, Smith BP, Walker F, Leon JM. Botulinum toxin type A neuromuscular blockade in the treatment of lower extremity spasticity in cerebral palsy: a randomized, double-blind, placebo-controlled trial. *J Pediatr Orthop* 2000;20:108–15.
- [2] Brouwer B, Davidson LK, Olney SJ. Serial casting in idiopathic toe-walkers and children with spastic cerebral palsy. *J Pediatr Orthop* 2000;20:221–5.
- [3] Javors JR, Klaaren HE. The Vulpius procedure for correction of equinus in cerebral palsy. *J Pediatr Orthop* 1987;7:191–3.
- [4] McDowell BC, Hewill V, Nurse A, Weston T, Baker R. The variability of goniometric measurements in ambulatory children with spastic cerebral palsy. *Gait Posture* 2000;12:114–21.
- [5] Gilja OH, Hausken T, Olafsson S, Matre K, Odegaard S. In vitro evaluation of three-dimensional ultrasonography based on magnetic scanhead tracking. *Ultrasound Med Biol* 1998;24(8):1161–7.
- [6] Blackall JM, Rueckert D, Maurer CR, Penney GP, Hill DLG, Hawkes DJ. An image registration approach to automated calibration for freehand 3D ultrasound. In: Proc. of medical image computing and computer assisted intervention (MICCAI) 2000. pp. 462–471.
- [7] Press WH, Teukolsky SA, Vetterling WT, Flannery BP. Numerical recipes in C. The art of scientific computing, 2nd ed.. Cambridge, UK: Cambridge University Press, 1992:408–12.
- [8] Wickiewicz TL, Roy RR, Powell PL, Edgerton VR. Muscle architecture of the human lower limb. *Clin Orthop* 1983;179:275–83.
- [9] Friederich JA, Brand RA. Muscle fibre architecture in the human lower limb. *J Biomech* 1990;23:91–5.
- [10] Lieber RL, Friden J. Functional and clinical significance of skeletal muscle architecture. *Muscle Nerve* 2000;23:1647–66.
- [11] Maganaris CN, Baltzopoulos V, Sargeant AJ. *In vivo* measurements of the triceps surae complex architecture in man: implications for muscle function. *J Physiol* 1998;512(Pt. 2):603–14.
- [12] Narici MV, Binzoni T, Hiltbrand E, Fasel J, Terrier F, Cerretelli P. *In vivo* human gastrocnemius architecture with changing joint angle at rest and during graded isometric contraction. *J Physiol* 1996;496:287–97.
- [13] Scott SH, Engstrom CM, Loeb GE. Morphometry of human thigh muscles. Determination of fascicle architecture by magnetic resonance imaging. *J Anat* 1993;182:249–57.
- [14] O'Dwyer NJ, Neilson PD, Nash J. Mechanisms of muscle growth related to muscle contracture in cerebral palsy. *Dev Med Child Neurol* 1989;31:534–7.
- [15] Shortland AP, Harris CA, Gough M, Robinson RO. Architecture of the medial gastrocnemius in children with spastic diplegia. *Dev Med Child Neurol* 2001;43:796–801.
- [16] Nelson TR, Downey DB, Pretorius DH, Fenster A. Three-dimensional ultrasound. Philadelphia: Lippincott Williams & Wilkins, 1999:28–9.
- [17] Gordon L. Anatomy and figure drawing. London: B T Batsford Limited, 1979:119.